

Supporting Information

Multiresponsive Nanoprobes for Turn-On Fluorescence/ ^{19}F -MRI Dual-Modal Imaging

Yawei Li¹, Hecheng Zhang², Chang Guo¹, Gaofei Hu^{1,*} and Leyu Wang^{1,*}

¹State Key Laboratory of Chemical Resource Engineering, Beijing Advanced Innovation Center for Soft Matter Science and Engineering, Beijing University of Chemical Technology, Beijing 100029, China; ²Dongzhimen Hospital, Beijing University of Chinese Medicine, Beijing 100700, China. Email: lywang@mail.buct.edu.cn (L.Y. W); hugf@mail.buct.edu.cn (G.F.H)

Table of Contents

Figure S1. XRD pattern of $\text{ZnS}:\text{Mn}^{2+}$ QDs (S2)

Figure S2. HRTEM images of $\text{ZnS}:\text{Mn}^{2+}\text{-F-Mn}(\text{OA})_2@\text{PSIOAm}$ before and after reaction with GSH (S2)

Figure S3. FT-IR spectra of $\text{ZnS}:\text{Mn}^{2+}$ QDs (the ligand is oleic acid), $\text{Mn}(\text{OA})_2$, PFCE, PSIOAm , and $\text{ZnS}:\text{Mn}^{2+}\text{-F-Mn}(\text{OA})_2@\text{PSIOAm}$ (S3)

Figure S4. UV-Vis absorption spectrum of $\text{Mn}(\text{OA})_2$, fluorescence spectra of $\text{ZnS}:\text{Mn}^{2+}@\text{PSIOAm}$ and $\text{ZnS}:\text{Mn}^{2+}\text{-Mn}(\text{OA})_2@\text{PSIOAm}$ (S3)

Figure S5. UV-Vis absorption of $\text{ZnS}:\text{Mn}^{2+}\text{-F}@\text{PSIOAm}$ and $\text{ZnS}:\text{Mn}^{2+}\text{-F-Mn}(\text{OA})_2@\text{PSIOAm}$ (S4)

Figure S6. ^{19}F NMR spectra of $\text{ZnS}:\text{Mn}^{2+}\text{-F-Mn}(\text{OA})_2@\text{PSIOAm}$ aqueous solution before and after reaction with GSH (10 mM) at pH 6.0 (S4)

Figure S7. UV-Vis absorption spectra and ICP-OES measurements of the Mn content in the supernatants of $\text{ZnS}:\text{Mn}(\text{OA})_2@\text{PSIOAm}$ colloidal solution at different conditions (S5)

Figure S8. Selectivity of $\text{ZnS}:\text{Mn}^{2+}\text{-F-Mn}(\text{OA})_2@\text{PSIOAm}$ toward GSH (S5)

Figure S9. Cytotoxicity tests of $\text{ZnS}:\text{Mn}^{2+}\text{-F-Mn}(\text{OA})_2@\text{PSIOAm}$ colloids after incubation with HUVECs and 4T1 cell lines (S6)

Figure S10. Flow cytometry analysis of MREpiC and 4T1 cells incubated with $\text{ZnS}:\text{Mn}^{2+}\text{-F-NLR-Mn}(\text{OA})_2@\text{PSIOAm}$ (S6)

Figure S11. Stability evaluation of $\text{ZnS}:\text{Mn}^{2+}\text{-F-Mn}(\text{OA})_2@\text{PSIOAm}$ colloid solution (S7)

Figure S12. T_1 -weighted and T_2 -weighted ^1H MR imaging of $\text{ZnS}:\text{Mn}^{2+}\text{-F-Mn}(\text{OA})_2@\text{PSIOAm}$ under different conditions (S7)

Figure S13. Fluorescence images of 4T1 cells cultured with $\text{ZnS}:\text{Mn}^{2+}\text{-F-Mn}(\text{OA})_2@\text{PSIOAm}$ nanoprobes for different time (S8)

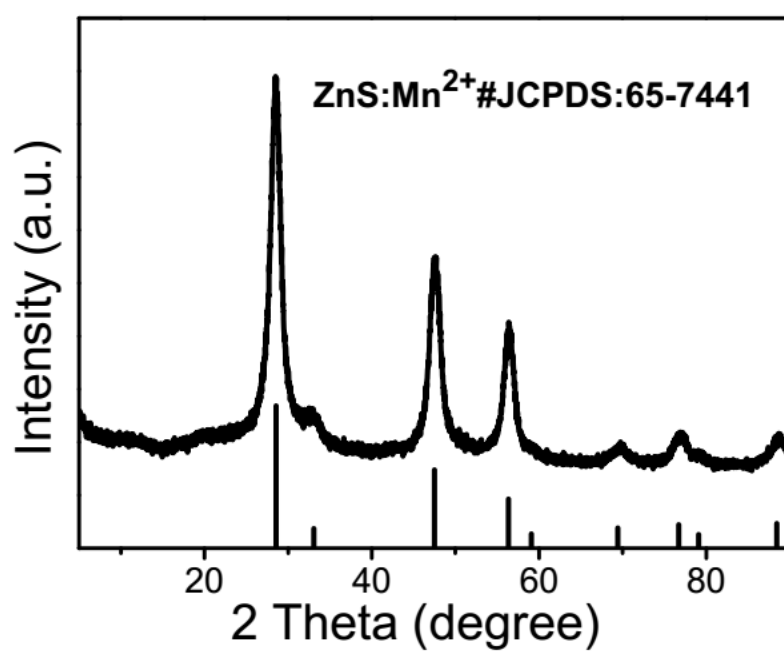


Figure S1. XRD pattern of ZnS:Mn²⁺ QDs.

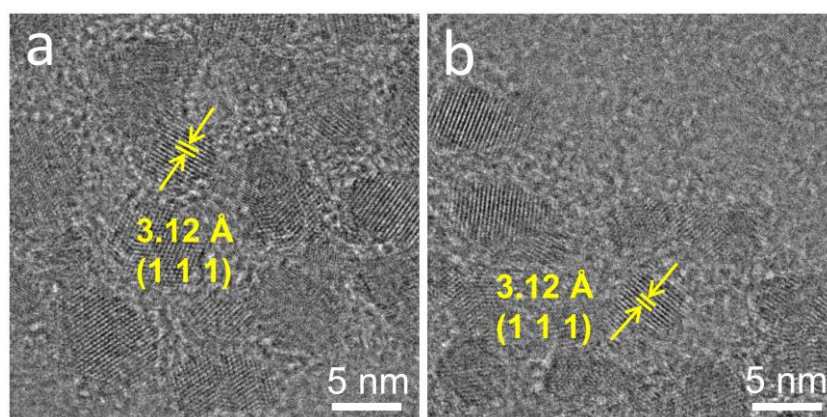


Figure S2. HRTEM images of ZnS:Mn²⁺-F-Mn(OA)₂@PSI_{oAm} nanoprobe before (a) and after (b) reaction with GSH (10 mM, at pH 6.0).

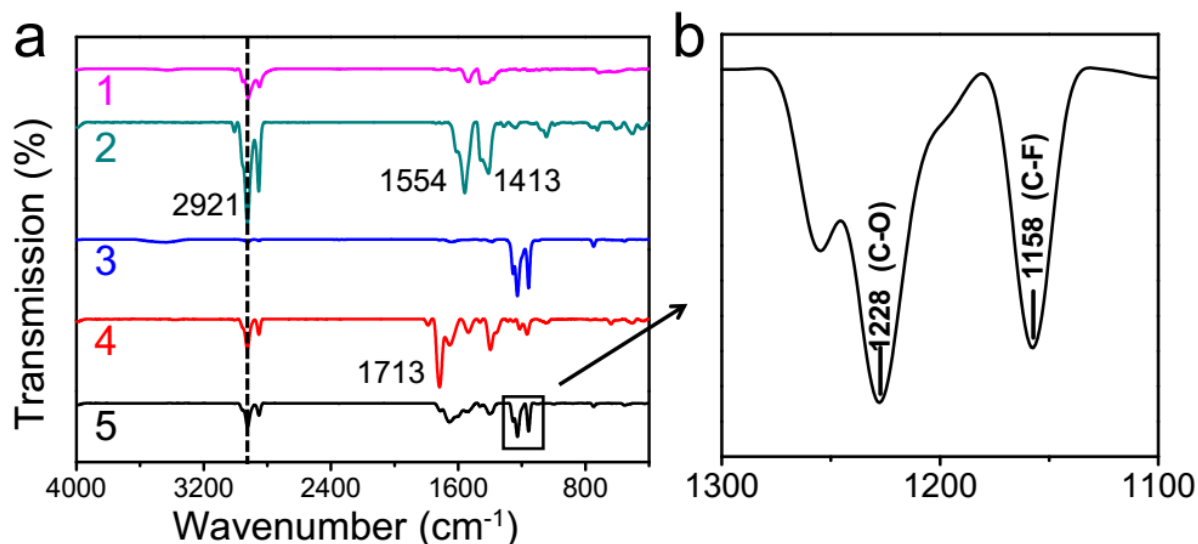


Figure S3. FT-IR spectra of different materials (1. ZnS:Mn²⁺ QDs, the ligand is oleic acid; 2. Mn(OA)₂; 3. PFCE; 4. PSIOAm; 5. ZnS:Mn²⁺-F-Mn(OA)₂@PSIOAm).

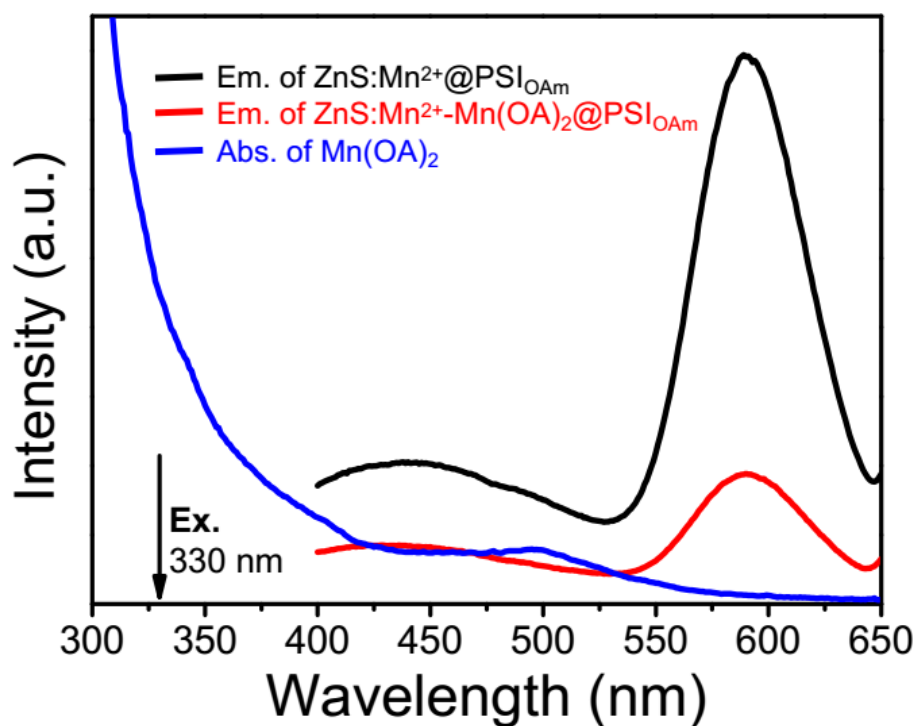


Figure S4. UV-Vis absorption spectrum of Mn(OA)₂, fluorescence spectra of ZnS:Mn²⁺@PSIOAm and ZnS:Mn²⁺-Mn(OA)₂@PSIOAm, respectively. Ex = 330 nm.

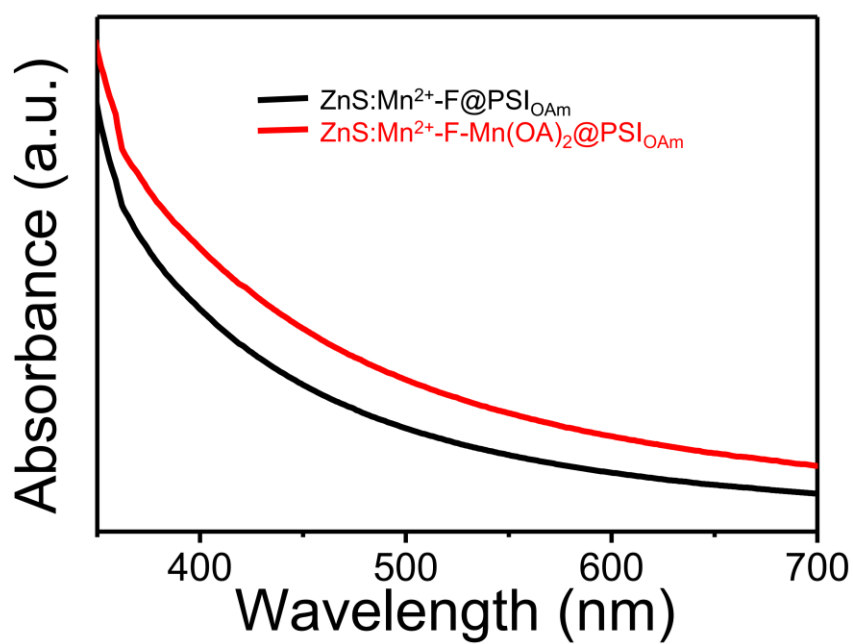


Figure S5. UV-Vis absorption spectra of ZnS:Mn²⁺-F@PSI_{OAm} and ZnS:Mn²⁺-F-Mn(OA)₂@PSI_{OAm}.

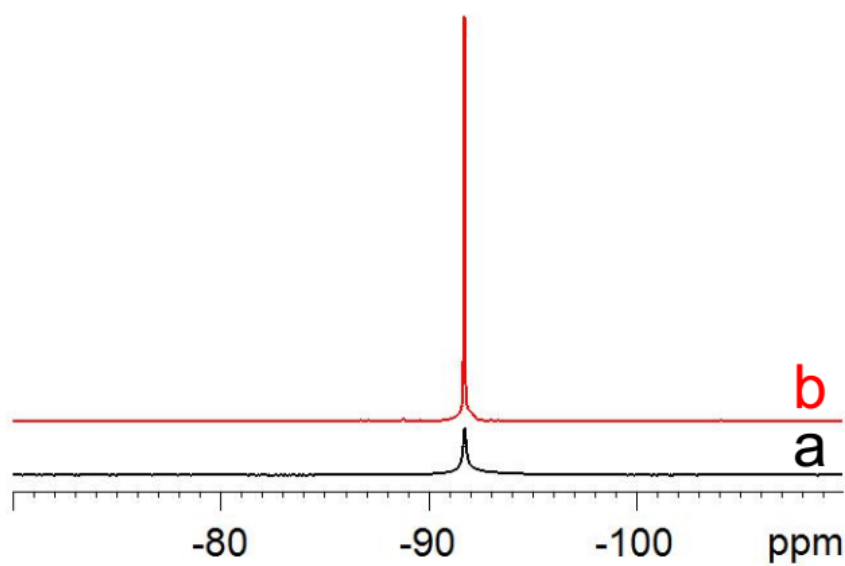


Figure S6. ¹⁹F NMR spectra of ZnS:Mn²⁺-F-Mn(OA)₂@PSI_{OAm} aqueous solution before (a) and after (b) reaction with GSH (10 mM) at pH 6.0, respectively.

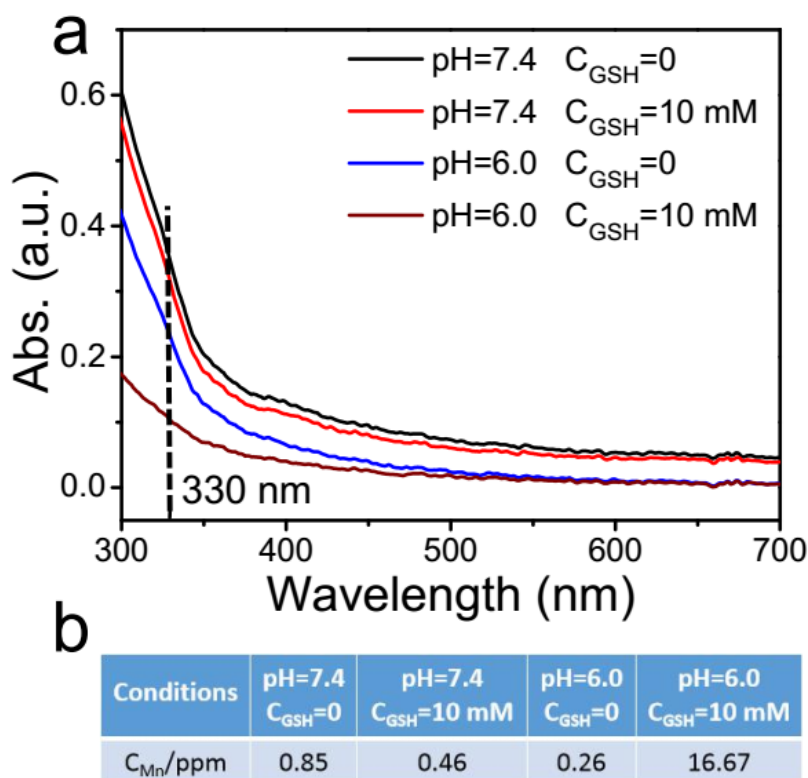


Figure S7. UV-Vis absorption spectra of ZnS-Mn(OA)₂@PSI_{OA}m colloidal solution at different conditions (a) and ICP-OES measurements of the Mn content (b) in the supernatants accordingly.

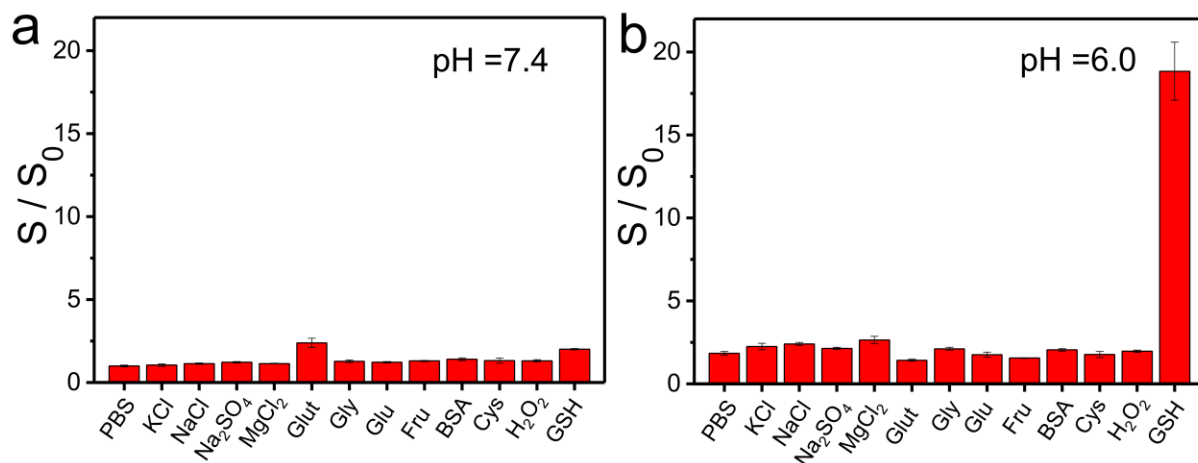


Figure S8. ¹⁹F NMR response (relative intensity, S/S₀) of ZnS:Mn²⁺-F-Mn(OA)₂@PSI_{OA}m toward various interference species under pH 7.4 (a) and pH 6.0 (b), respectively. The concentration of bovine serum albumin (BSA) was 1.0 mg/mL, the others were 10 mM. Glut, Gly, Glu, Fru, and Cys refer to glutamic acid, glycine, glucose, fructose, and cysteine, respectively. For each group, three independent parallel experiments were carried out (n = 3).

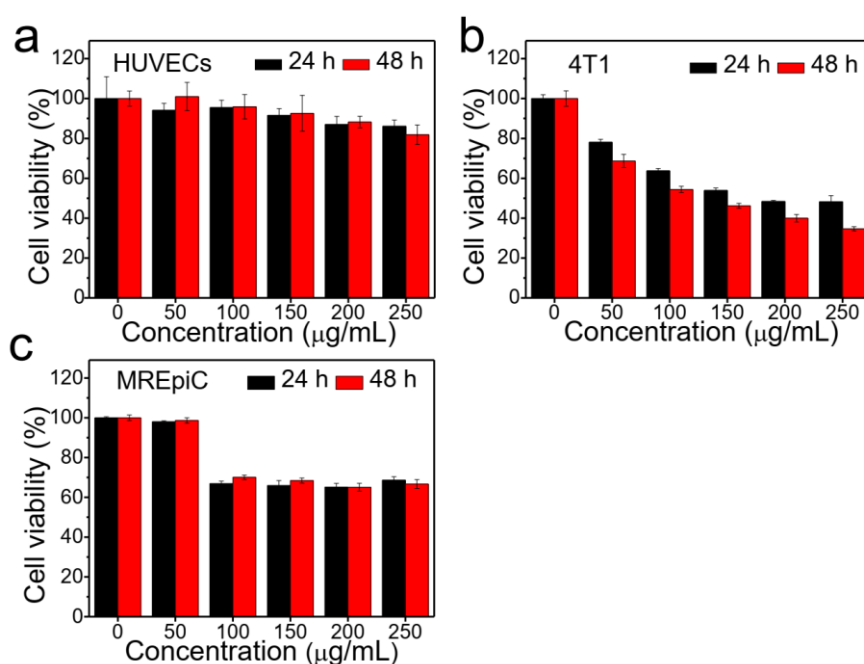


Figure S9. Cytotoxicity tests of $\text{ZnS:Mn}^{2+}\text{-F-Mn(OA)}_2\text{@PSIOAm}$ colloids after incubation with HUVECs cells (a), 4T1 cells (b) and MREpiC cells (c) for 24 h and 48 h, respectively. For each concentration level, six independent parallel experiments were carried out ($n = 6$).

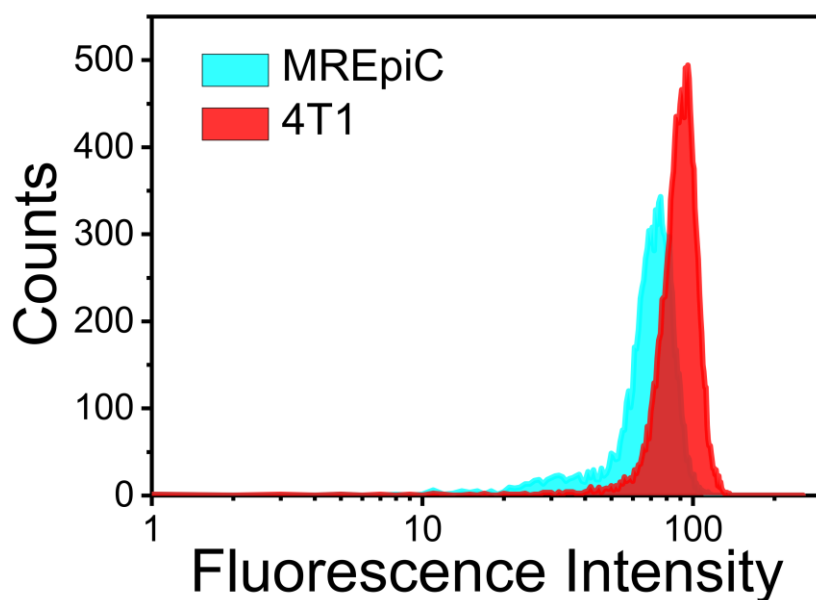


Figure S10. Flow cytometry analysis of MREpiC and 4T1 cells incubated with $\text{ZnS:Mn}^{2+}\text{-F-NLR-Mn(OA)}_2\text{@PSIOAm}$ for 4 h. The excitation and emission wavelengths were 488 nm and 630 nm, respectively. (Note: Nile red (NLR) loading was required because its excitation wavelength (~ 480 nm) also lies in the range of the absorption of Mn(OA)_2 , meanwhile suitable for FC analysis).

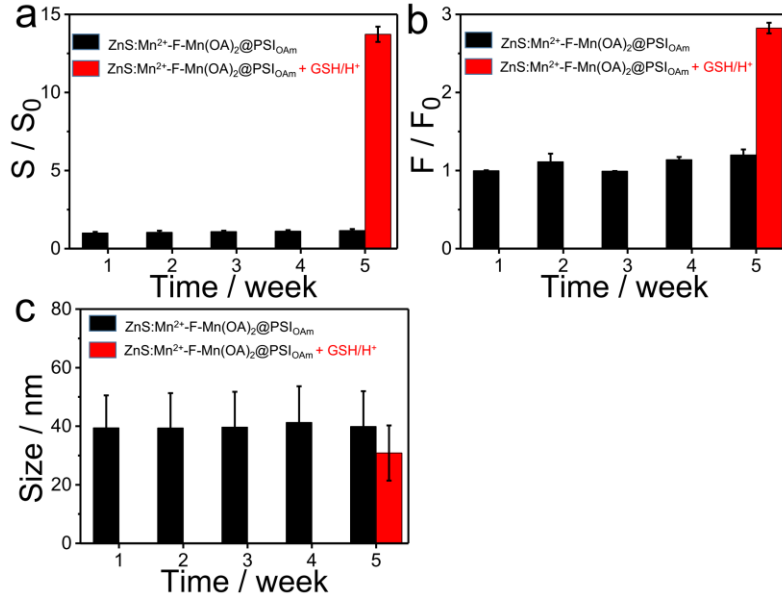


Figure S11. Stability evaluation of ZnS:Mn²⁺-F-Mn(OA)₂@PSIOAm colloids by observing the evolution of ¹⁹F MR signal (a), fluorescence (b) and DLS size (c) versus time, respectively. S₀ and F₀ refer to ¹⁹F MR signal and fluorescence intensity of the first measurement, namely, the freshly prepared sample solution (pH 7.4). For each measurement, 400 μ L of the sample solution was mixed with 500 μ L of PBS buffer solution with different pH values (pH 6.0 for GSH groups, otherwise pH = 7.4). C_{GSH} = 10 mM. For each time interval, three independent parallel experiments were carried out (n = 3).

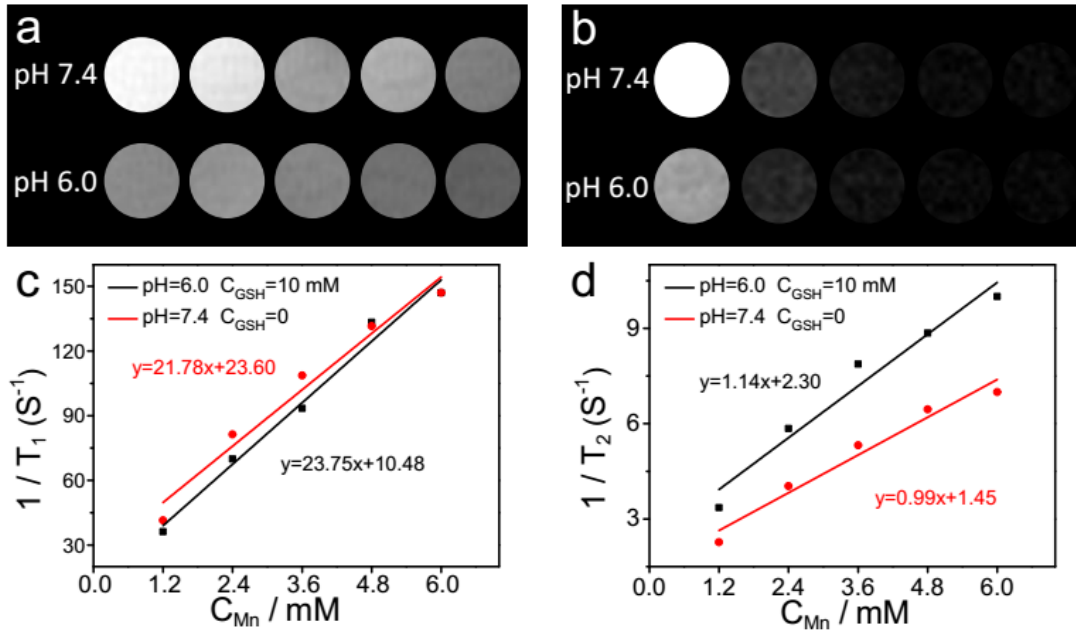


Figure S12. T₁-weighted (a) and T₂-weighted (b) ¹H MR imaging of ZnS:Mn²⁺-F-Mn(OA)₂@PSIOAm with different concentrations diluted from samples under pH 7.4, C_{GSH} = 0, and pH 6.0, C_{GSH} = 10 mM, respectively. The corresponding longitudinal (c) and transverse (d) relaxation rate evolution profile versus concentration of total Mn.

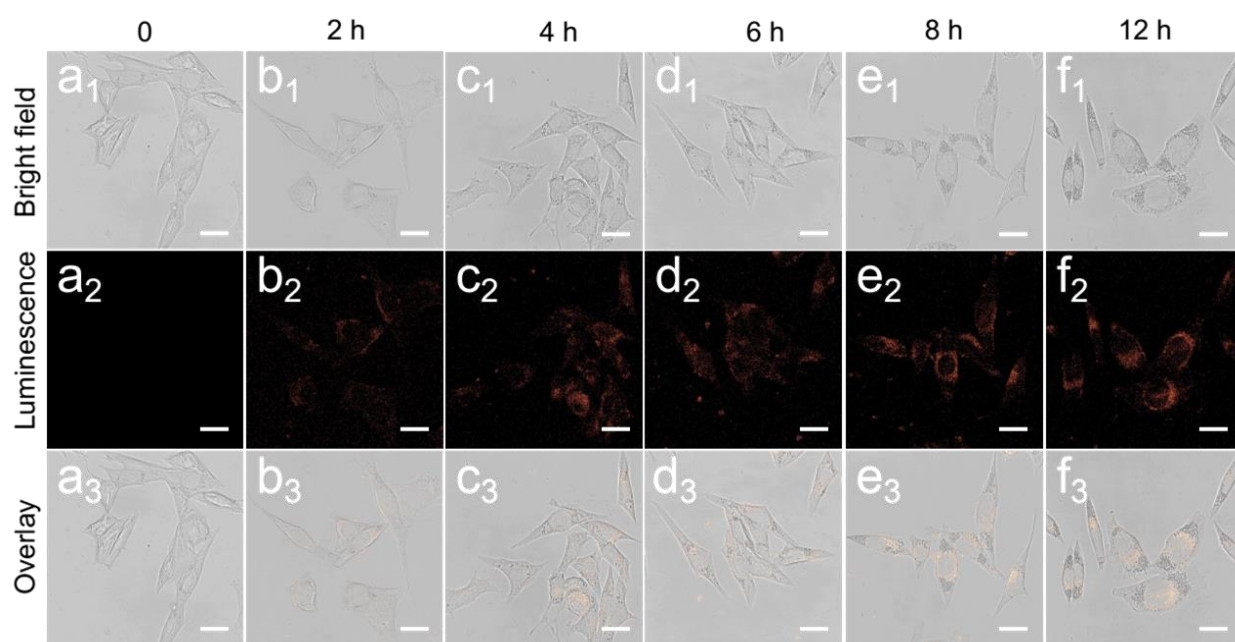


Figure S13. Fluorescence images of 4T1 cells cultured with $\text{ZnS:Mn}^{2+}\text{-F-Mn(OA)}_2\text{@PSI}_{\text{OAm}}$ nanoprobe for different time. The scale bars in the figure are 25 μm .